PNAS
www.pnas.org

Supplementary Information for

Mechanical fatigue of human red blood cells

Yuhao Qiang, Jia Liu, Ming Dao*, Subra Suresh*, E Du*

*Ming Dao, E-mail: mingdao@mit.edu
*Subra Suresh, E-mail: ssuresh@ntu.edu.sg
*E Du, E-mail: edu@fau.edu

This PDF file includes:

Supplementary text
Figs. S1 to S9
Table S1
Captions for Movies S1 to S4
References for SI reference citations

Other supplementary materials for this manuscript include the following:

Movies S1 to S4

Supplementary Information

Experimental Setup. The microfluidic chip designed for conducting the fatigue test consists of a 50 μm deep, 500 μm wide and 10 mm long polydimethylsiloxane (PDMS) microfluidic channel and two interdigitated electrodes (with 20 μm gap and 20 μm band width) coated on 0.7 mm thick glass. The electrical excitation system consists of a printed circuit board (PCB) with a microscopic observation area and a signal generator (SIGLENT SDG830, SIGLENT, P.R. China). Red blood cell (RBC) deformation was observed through a high-resolution CMOS camera (The Imaging Source, Charlotte, NC) which is mounted on an Olympus X81 inverted microscope (Olympus America, PA, USA), where image contrast was enhanced by inserting a 414 ± 46 nm band pass filter in the optical path. The microfluidic channel was coated with dielectrophoresis (DEP) buffer solution with 5% bovine serum albumin (BSA, Lot 20150520AS, Rocky Mountain Biologicals. Inc, Missoula, MT) for more than 30 min before each test, so as to prevent adhesion of the cell to the bottom of the channel. Any excess coating medium in the channel was then removed along with the DEP buffer before the cell suspension was injected into the microfluidic chip.

Sample Preparation. Blood samples from healthy donors were obtained with institutional review board (IRB) approval from Florida Atlantic University. All blood samples used were de-identified prior to use in the study. The DEP buffer was prepared by mixing 8.5% (w/v) sucrose and 0.3% (w/v) dextrose in deionized water, and further adjusting electrical conductivity to 0.02 S/m using phosphate buffered saline (PBS) solution (Lonza Walkersville, Inc., Walkersville, MD). Prior to each fatigue test, blood samples were gently washed twice with PBS at 2,000 rpm for 2 min at room temperature. The RBC pellet was collected and re-suspended in the DEP buffer to a final concentration of 10^6 cells/ml.

Statistical Study. RBCs were individually tracked as a function of time during the course of the experiments. Statistical analyses were performed using OriginPro 9 (OriginLab, Northampton, MA). All data were expressed in terms of statistical mean ± SD, except stated otherwise. A paired *t*-test between measurements of samples from the initial cycle and subsequent cycles was used to generate *p* values. A two-sample *t*-test was used to generate the *p* values between measurements for different loading cases. The *p* values equal to or smaller than 0.05 were considered statistically significant differences between the results that were compared. For correlation studies, R^2 (the *R*-squared values) are listed.

Electro-deformation Characterization of RBCs

As a result of interfacial Maxwell–Wagner polarization across the cellular membrane (1), the RBC is subjected to a DEP force from the dipole moment induced by a non-uniform electric field. The direction and magnitude of the DEP force depend on the electrical properties of the cell and the surrounding medium as well as the on the amplitude and frequency of the electric field. Assuming that the shape of RBC can be approximated as an ellipsoid, the time-averaged DEP force can be quantified by (1)

$$\langle F_{\mathrm{DEP}} \rangle = \frac{\pi}{4} abc \cdot \epsilon_{\mathrm{m}} \cdot Re(f_{\mathrm{CM}}) \cdot \nabla E_{\mathrm{rms}}^2 \tag{1}$$

where *a*, *b* and *c* are the dimensions along *x*, *y* and *z* axes of the RBC, respectively; ϵ_{m} is the permittivity of the surrounding medium, and ∇E_{rms} the root-mean-square of the gradient of electric field strength. The direction of electro-deformation force exerted on the RBC is determined by the value of the real part of the Clausius Mossotti factor (f_{CM}), $Re(f_{\mathrm{CM}})$. When $Re(f_{\mathrm{CM}})$ is positive, the cells move toward the electrode, and eventually get trapped at the electrode edges under positive electro-deformation. Conversely, under negative DEP ($Re(f_{\mathrm{CM}}) < 0$), the cells are repelled from the electrodes. The value of f_{CM} can be estimated using a concentric multi-shell model (2, 3),

$$f_{\mathrm{CM}} = \frac{1}{3} \frac{(\epsilon_{\mathrm{mem}}^* - \epsilon_{\mathrm{m}}^*)[\epsilon_{\mathrm{mem}}^* + A_1(\epsilon_{\mathrm{cyto}}^* - \epsilon_{\mathrm{mem}}^*)] + \rho(\epsilon_{\mathrm{cyto}}^* - \epsilon_{\mathrm{mem}}^*)[\epsilon_{\mathrm{mem}}^* - A_1(\epsilon_{\mathrm{mem}}^* - \epsilon_{\mathrm{m}}^*)]}{(\epsilon_{\mathrm{m}}^* + A_1(\epsilon_{\mathrm{mem}}^* - \epsilon_{\mathrm{m}}^*))\left[\epsilon_{\mathrm{mem}}^* + A_1(\epsilon_{\mathrm{cyto}}^* - \epsilon_{\mathrm{mem}}^*)\right] + \rho A_2(1 - A_2)(\epsilon_{\mathrm{cyto}}^* - \epsilon_{\mathrm{mem}}^*)(\epsilon_{\mathrm{mem}}^* - \epsilon_{\mathrm{m}}^*)} \tag{2}$$

where the subscripts mem, m and cyto represent membrane, medium and cytoplasm, respectively. $\epsilon^* = \epsilon - \mathrm{j}\delta/\omega$, where ω, ϵ and δ are the angular frequency, dielectric permittivity and conductivity, respectively. $\rho = (a-d)(b-d)(c-d)/(abc)$, where *d* denotes the thickness of the cell membrane. $A_{i=1,2}$ is the depolarization factor, defined as

$$A_i = \frac{a_i b_i c_i}{2} \int_0^\infty \frac{ds}{(s+a_i^2)B_i}, i = 1, 2 \quad (3)$$

where s is a dummy integration variable, $B_i = \sqrt{\left((s+a_i^2)(s+b_i^2)(s+c_i^2)\right)}$, $a_1 = a$, $b_1 = b$, $c_1 = c$, $a_2 = a - d$, $b_2 = b - d$, and $c_2 = c - d$.

Table S1. Typical values of parameters used in the calculation of $Re(f_{CM})$ of healthy RBCs(4, 5)

Cell	*a* (μm)	*b* (μm)	*c* (μm) (4)	*d* (nm) (5)	ϵ_{mem} (5)	δ_{mem} (S/m) (5)	ϵ_{cyto} (5)	δ_{cyto} (S/m) (5)	ϵ_{m}	δ_{m} (S/m)
Healthy RBCs	8	8	2.6	4.5	4.44	10^{-6}	59	0.31	80	0.02

As shown in Fig. S1A, $Re(f_{\text{CM}})$ was calculated as a function of the electrical frequency using Eq. (2) based on the geometrical parameters and properties of healthy RBCs, which are available from the literature (4, 5) (Table S1). For the chosen frequency of 1.58 MHz in our experiment, electrical excitation provides a favorable positive DEP effect on RBCs. To evaluate the influence of possible variations in DEP on RBCs, we performed parametric analysis of $Re(f_{\text{CM}})$ by multiplying the electrical properties of subcellular components in Table S1 with a factor, k. $Re(f_{\text{CM}})$ decreased from 1.252 to only 1.247 as k increased from unity to 2 for membrane conductivity, δ_{mem} (Fig. S1B). The value of $Re(f_{\text{CM}})$ slightly decreased from 1.253 to 1.249 when k ranged from 0.5 to 2 for cytoplasm permittivity, ϵ_{cyto} (Fig. S1C). These results show that $Re(f_{\text{CM}})$ is not sensitive to δ_{mem} and ϵ_{cyto}. It should also be noted that the value of $Re(f_{\text{CM}})$ increased from 0.96 to 1.44, as k ranged from 0.5 to 2 for cytoplasm conductivity, δ_{cyto} (Fig. S1D). Assuming a linear variation between the hemoglobin concentration and cytoplasmic conductivity, we find that $Re(f_{\text{CM}})$ is also not very sensitive to cytoplasmic conductivity.

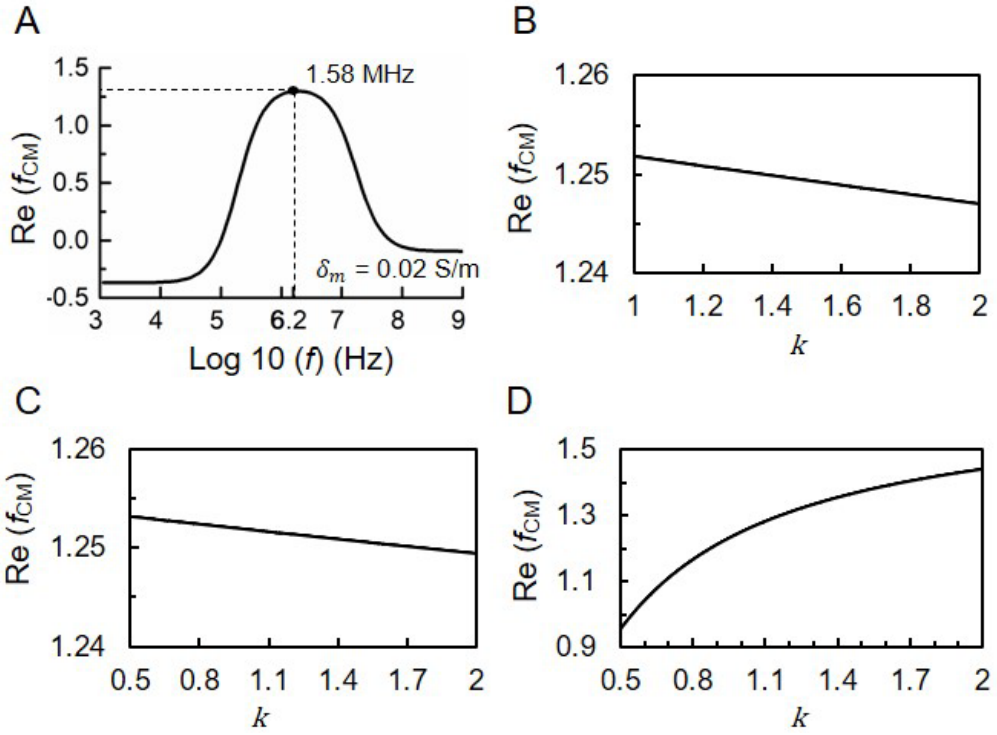

Fig. S1. Parametric analysis of DEP behavior of RBCs: (A) $Re(f_{\text{CM}})$ of healthy RBCs as a function of electrical frequency in the working medium with conductivity of 0.02 S/m. (B-D) $Re(f_{\text{CM}})$ of RBCs as functions of factor k for membrane conductivity, cytoplasm permittivity, and cytoplasm conductivity, respectively.

The Maxwell stress tensor (MST) method was used to calculate the electro-deformation force using the finite element analysis package COMSOL Multiphysics (Burlington, MA, USA). Here, the effects of cells on the distribution of electrical field was taken into account since cells have a size comparable to that of the electrodes and move toward the electrodes under positive DEP. The time-averaged tensor is given by (6)

$$\langle \boldsymbol{\sigma}^{\mathrm{MST}} \rangle = \frac{1}{4} Re[\tilde{\epsilon}](\boldsymbol{E}\boldsymbol{E}' + \boldsymbol{E}'\boldsymbol{E} - |\boldsymbol{E}|^2 \boldsymbol{I}) \tag{4}$$

$$\langle \boldsymbol{F} \rangle = \oint_S \langle \boldsymbol{\sigma}^{\mathrm{MST}} \rangle \cdot \boldsymbol{n} dS \tag{5}$$

where $\tilde{\epsilon}$ denotes the complex electrical permittivity, $\boldsymbol{E}$ the electrical field, $\boldsymbol{I}$ the unit second-order tensor, and the product of two vectors results in the dyadic product. S is the outer surface area of the cell, and $\boldsymbol{n}$ is the unit vector normal to the cell surface.

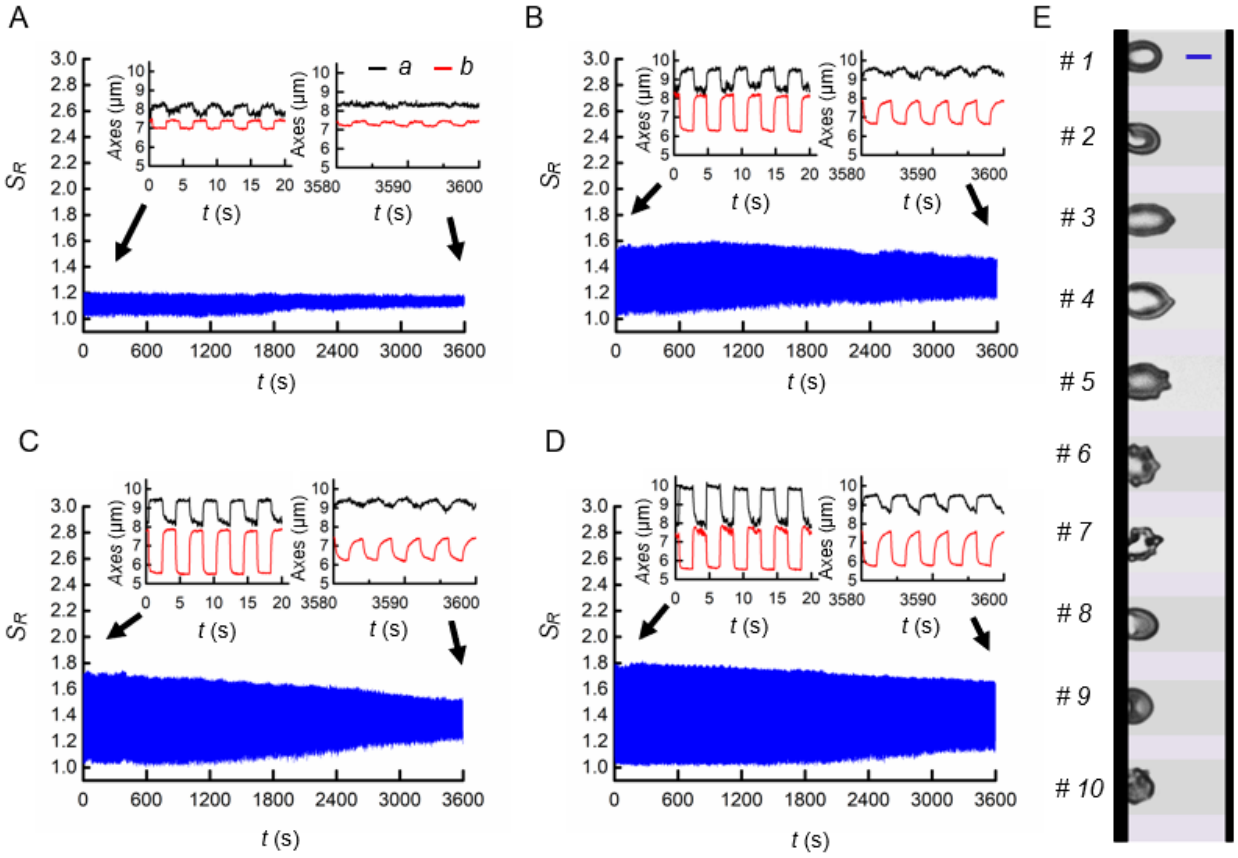

Fig. S2. Fatigue characteristics of RBCs in response to cyclic tensile loading with rectangular waveform for load ratio, R = 0 at variable voltage levels. (A-D) Quantitative measurements of the stretch ratio, S_R, as a function of time, for different representative cells in response to 0.5 V, 0.8 V, 1.0 V and 1.2 V, respectively. Insets indicate major and minor axes, *a* and *b* of ellipse-fitted cell shapes during the initial five and last five cycles (left and right insets, respectively). (E) Formation of permanent damage in cell membrane during cyclic loading: Cell # 1 after N = 855 at a peak load of 0.8 V, Cell # 2 after N = 250 at 1.0 V, Cell # 3 after N = 330 at 1 V, Cell # 4 after N = 185 at 2.0 V, Cell # 5 after N = 533 at 0.8 V, Cell # 6 after N = 100 at 1.5 V, Cell # 7 after N = 900 at 2.0 V, Cell # 8 after N = 360 at 1.5 V, Cell # 9 after N = 868 at 2.0 V, and Cell # 10 after N = 834 at 1 V. (Scale bars in E denote a length scale of 5 μm).

The evolution of the stretch ratios, S_R, from cyclic electro-deformation for four representative RBCs at different voltages of 0.5 V, 0.8 V, 1.0 V, and 1.2 V are plotted against time in Fig.S2*A*–*D*, respectively. In response to cyclic tensile loading, S_R values of cell membranes exhibit in-phase cyclic deformation patterns that are enveloped by upper and lower bound values. The envelope of maximal S_R represents the maximum deformation during each cycle and descends gradually with fatigue cycles; the bound of minimum S_R represents the fully relaxed cell membranes and its value increases gradually with fatigue cycles. The two bounds tend to approach each other, indicating the gradual hardening process and irreversible deformation in cell membranes with the progression of fatigue. The differences between the two bounds increase with the amplitude of the applied voltage. The insets in each plot in Fig. S2 indicate variations in the values of major and minor axes (*a* and *b,* respectively) of the RBC during the first five and last five cycles, for each of the four cell examples.

Constitutive Model for Viscoelastic Deformation of RBC Membranes

In response to shear stresses induced by the application of an electrical voltage, the RBC membrane exhibits viscoelastic deformation. Such behavior has been idealized using a time-dependent constitutive behavior described by the Kelvin-Voigt solid model (7, 8). For instance, under constant-amplitude cyclic electro-deformation loading, RBC membranes undergo viscoelastic behavior during each cycle of tensile-stretching and relaxation.

The transient extension ratio $\lambda(\mathrm{t})$ is defined as the ratio of the initial value of minor axis b_0 of the ellipse representing the shape of the RBC to the instantaneous value of the minor axis $b(t)$ at any time t in both the stretching and relaxation phases of fatigue. Note that $\lambda(t)$ is defined as $b_0/b(t)$ and not in terms of the longer-axis extension ratio, $a(t)/a_0$, because a small part of deformed membrane along the major axis, *a,* is necessarily obstructed from view by the gold electrode when imaging the cell, and this could lead to an error in the calculation if the latter definition of $\lambda(\mathrm{t})$ had been invoked. In a later section of this *SI Appendix*, we demonstrate that the definition of the instantaneous values extension ratio based either on the axial stretch, $a(t)/a_0$, or the corresponding transverse contraction, $b_0/b(t)$, has no effect on the trends discovered here about the role of mechanical fatigue in influencing the behavior of RBCs. The actual values of $\lambda(t)$ vary as anticipated because of the normal variations in cell response and experimental scatter in extracting axial and transverse dimensions during deformation from optical images.

The resulting shear strain ε is calculated as

$$\varepsilon(t) = \frac{(\lambda(t)^2 - \lambda(t)^{-2})}{2} \tag{6}$$

Specifically, transient shear stress σ from electro-deformation loading is determined by

$$\sigma(t) = \frac{F(t)}{2b(t)} \tag{7}$$

Thus, transient stress versus deformation relationship of single RBCs can be written according to the Kelvin-Voigt solid model, by combining Eqs. (6) and (7), as

$$\frac{\sigma(t)}{2\mu} = \frac{1}{4}(\lambda(t)^2 - \lambda(t)^{-2}) + t_c \frac{\partial \ln \lambda(t)}{\partial t} \tag{8}$$

where μ is the membrane shear modulus, $t_c \equiv \eta/\mu$ is the characteristic time for relaxation which is a material time constant, and η is shear viscosity. Value of t_c can be extracted from an exponential fit of the data of $\lambda(t)$ during the relaxation phase (when $\sigma = 0$),

$$\exp\left(-\frac{t}{t_c}\right) = \frac{(\lambda - \lambda_0)(\lambda_{\max} + \lambda_0)}{(\lambda + \lambda_0)(\lambda_{\max} - \lambda_0)} \tag{9}$$

where $\lambda_{\max}$ and λ_0 represent the values of λ measured in the fully-stretched and fully-relaxed states, respectively.

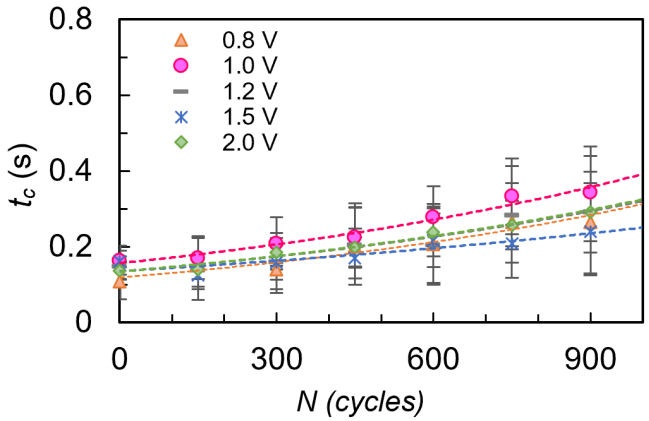

Fig. S3. The characteristic time of relaxation, t_c, of healthy RBCs for five different voltage levels, *V*, are plotted. The symbols denote experimental results of relaxation time calculated using Eq. (9). The dashed lines present the fit using an exponential function for each value of the voltage applied to the cells.

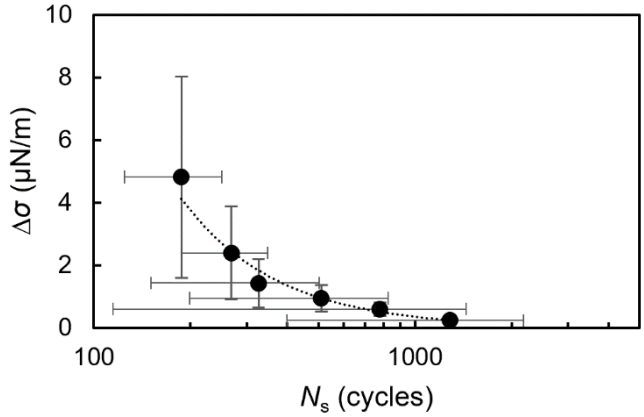

Fig. S4. The *S-N* diagram obtained from the fatigue testing of RBCs (*n* = 20). Here the number of cycles to life, N_s, is defined as that leading to a 5% reduction in λ_{max} as a result of cyclic loading and accumulated damage. The dashed curve represents the best fitting function to the Wöhler equation, $\Delta\sigma = 9184.2 \times (N_s)^{-1.473}$. Best fitting function for the Wöhler equation, $\Delta\sigma = \sigma_f \times (N_s)^b$ for the *S-N* data provides the strength factor, $\sigma_f = 9184\ \mu\mathrm{N/m}$, and the Basquin exponent, $b = -1.743$.

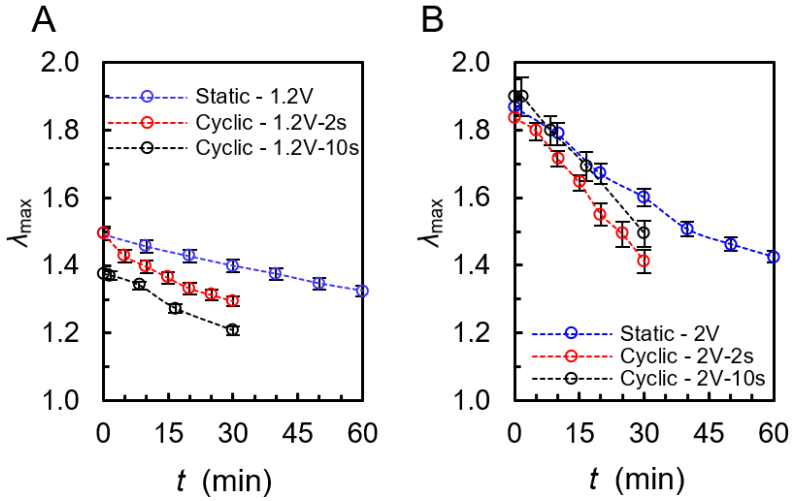

Fig. S5. Reduction of maximum deformation of cells as a function of accumulated loading time under static loading and cyclic loading: (A) Applied voltage of 1.2 V static loading (*n* = 35, blue circles), 1. 2 V–2 s cyclic loading (*n* = 58, red circles), and 1. 2 V–10 s cyclic loading (*n* = 49, black circles) (B) 2.0 V static loading (*n* = 27, blue circles), 2 V–2 s cyclic loading (*n* = 20, red circles), and 2 V–10 s cyclic loading (*n* = 40, black circles). Error bars indicate SEM.

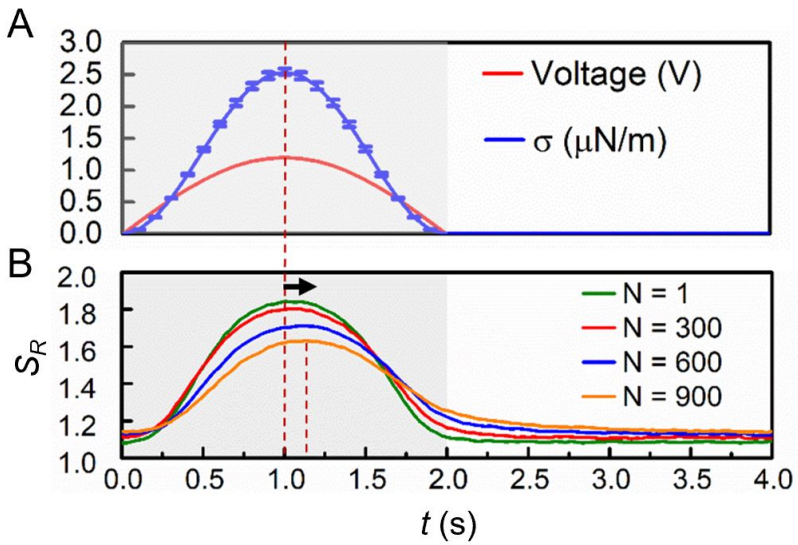

Fig. S6. An HWR sinusoidal waveform electrical excitation (red curve) and consequent shear stress averaged from the number of fatigue cycles, N = 1, 300, 450, 600, 900 (blue curve). The vertical red dashed line indicates the location of the peak value of voltage and membrane stress. (B) Instantaneous S_R averaged from individually tracked cells (n = 22) in both loading phase (gray region) and unloading phase (white region) at different fatigue cycles for the HWR sinusoidal waveform.

RBC Viability Assay

RBC viability was investigated by recourse to LIVE/DEAD® Viability/Cytotoxicity Kit (Invitrogen™ L3224, Thermo Fisher Scientific, Carlsbad, CA) staining of the green-fluorescent calcein-AM to indicate intracellular esterase activity. The assay was performed according to the manufacturer's protocol with a modification of the recommended buffer with DEP buffer, for which the osmotic pressure and pH value are similar to those of the cytoplasm of healthy RBCs. This replacement was done to ensure that no additional stress was imposed on the cells following fatigue testing. Cell viability results has been verified by identical viability results obtained for healthy RBCs prior to fatigue testing using the PBS buffer and the DEP buffer in parallel analyses. Considering the higher sample volume required by the LIVE/DEAD assay than the volume available (2.5 x10^{-6} mL) in the microfluidic device, we used a commercial 16-well plate (cat. No. 6324738001, ACEA Biosciences, San Diego, CA). The embedded interdigitated electrodes allowed us to obtain the required sample volume of RBCs (10 wells) that are subjected to simultaneous fatigue testing, equivalent to 1. 2 V–2 s loading and unloading as reported in the main paper. Each well was loaded with 200 μL of RBC suspension (10^6 cells/mL) in the DEP buffer and subjected to simultaneous cyclic electro-deformation for 1 h. The cyclic loading results of RBCs in the plate were consistent to the results obtained with cyclic loading our *in vitro* microfluidic device. Cells were collected after fatigue testing and stained with the viability assay, following the procedure stated in the manufacturer's protocol. Green fluorescence of the cells (Fig. S7A) was monitored by using a standard band pass filter with a wavelength of 475 nm, and compared to bright field image of the same of view of cells (Fig. S7B). Cell viability, defined as the percentage of cells that are viable, was not impacted by DEP buffer for long-term incubation under stationary condition. Initial cell viability before the fatigue testing was 100%. The fatigued RBCs showed an overall viability of 98±2% measured from 19 sets of fluorescence and bright field images.

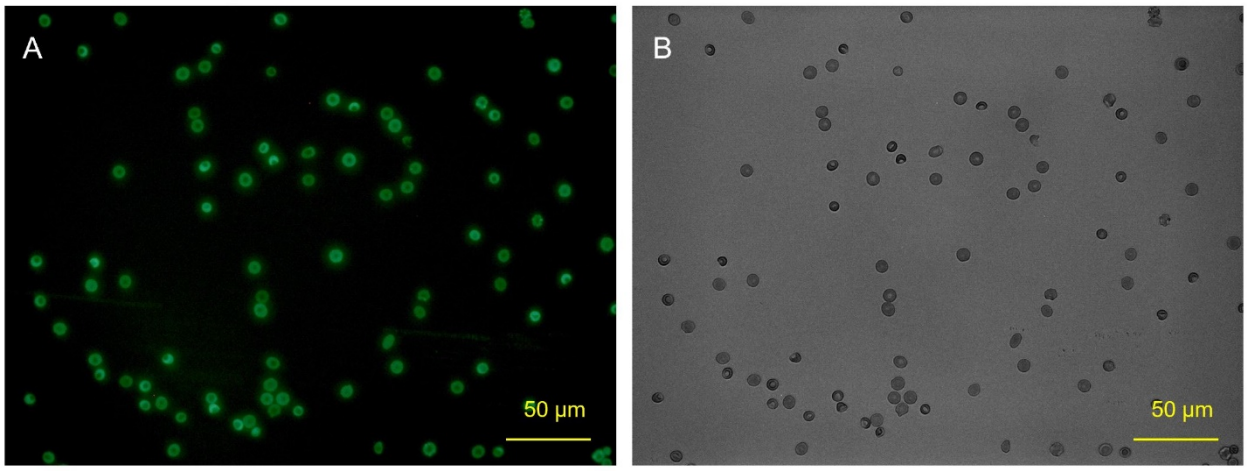

Fig. S7. RBC viability analysis by comparing the microscopic images of (A) green-fluorescent calcein-AM and (B) bright field image of the same field of view.

Axial versus Transverse Measurements of Deformation

As noted in the main paper, the principal extension ratio, $\lambda(t)$, was calculated by dividing the initial value of minor axis (b_0) by its transient value ($b(t)$). This choice of definition, instead of choosing the axial extension ratio, $a(t)/a_0$, was based on the consideration that a small part of deformed membrane along the tensile loading axis, *a,* is necessarily obstructed from view by the gold electrode when imaging the cell. This partial obstruction of view while imaging could have led to some errors in determining the extension ratio had $\lambda(t)$ been defined in terms of the relative stretch along the axial direction. We have determined experimentally that the choice of either of the two foregoing definitions would have absolutely no bearing on the trends and conclusions reported in this work. As expected, however, there are some differences in the results between these two related definitions of $\lambda(t)$, which stem from normal variations in cell responses in the two principal directions and differences in the accuracy of optical imaging between the two directions.

Fig. S8 demonstrates how the results presented in Fig. 4A would change had the extension ratio been defined as $\lambda(t) = a(t)/a_0$, instead of as $\lambda(t) = b_0/b(t)$, for static and cyclic loading. Here, Fig. S8A replots the results of Fig. 4A showing the variation of $\lambda^*_{\max}$ as a function of time for 1.2 V static loading and 1. 2 V–2 s for cyclic loading for $\lambda(t) = b_0/b(t)$, and compares it to the results, shown in Fig. S8B, for the same conditions with $\lambda(t) = a(t)/a_0$. It is evident here that the greater loss of deformability under cyclic loading is demonstrated in both cases. Effects of the two different means of assessing $\lambda(t)$ on the characterized mechanical fatigue of RBCs under 1.2 V static loading (n = 20) and 1.2 V-2 s cyclic loading (n = 35) are illustrated in Fig. S9. The characteristic time of relaxation, t_c, also increases with increasing number of fatigue cycles (see Fig. S3), irrespectively of whether deformation is quantified in terms of axial extension ratio or transverse contraction ratio.

We conclude, based on the results of Figs. S8 and S9 and other detailed results comparing the extension ratios in the two orthogonal directions, that estimates of principal deformation predicated either on the axial extension ratio, $a(t)/a_0$, or transverse contraction ratio, $b_0/b(t)$, has no effect on the trends discovered here about the role of mechanical fatigue in influencing the behavior of RBCs, despite some numerical differences in the extent of changes in behavior.

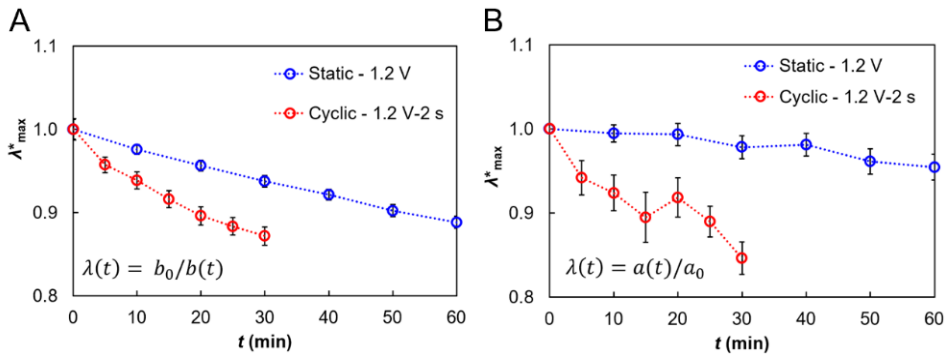

Fig. S8. A comparison of the static loading (n = 35) vs. cyclic loading (n = 20) effects on the deformability of RBCs using two different means of assessing the maximum extension ratio. (A) For $\lambda(t) = b_0/b(t)$, and (B) for $\lambda(t) = b(t)/b_0$. Error bars indicate SEM.

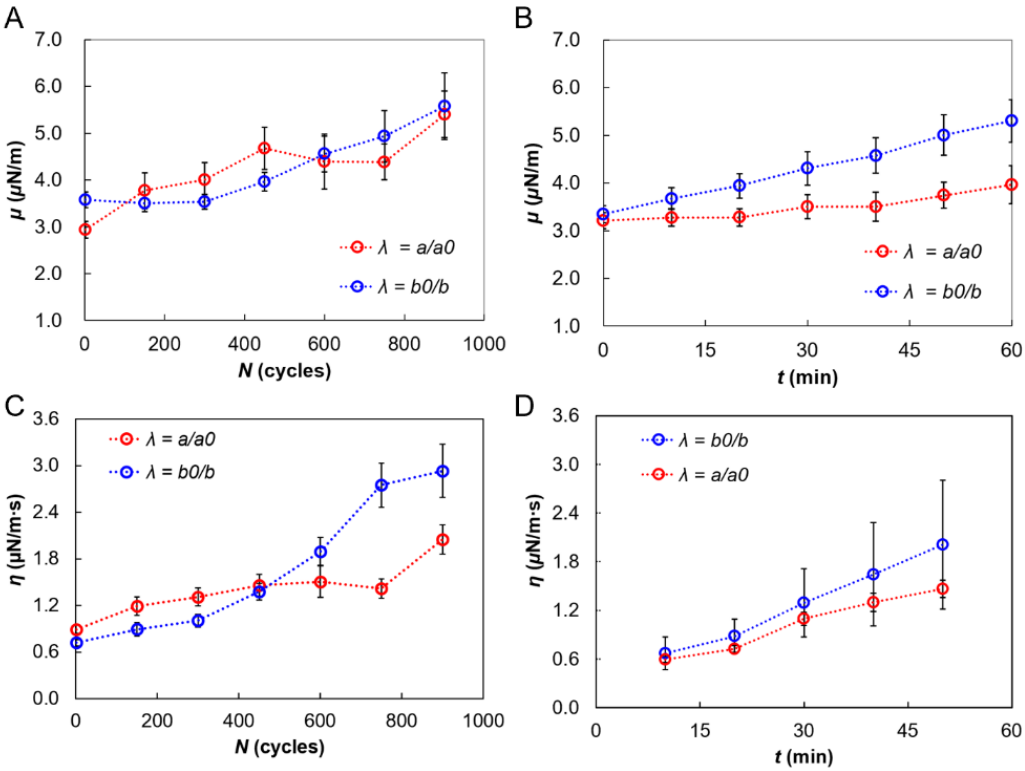

Fig. S9. Comparison between the two different means of assessing of the extension ratio, $\lambda(t) = b_0/b(t)$ and $\lambda(t) = a(t)/a_0$, for characterizations of (A) shear modulus, μ, under 1.2 V-2s cyclic loading, (B) shear modulus, μ, under 1.2 V static loading, (C) viscosity, η, under 1.2 V-2s cyclic loading, and (D) viscosity, η, under 1.2 V static loading. Error bars indicate SEM.

Movie S1. RBCs respond to a rectangular-waveform cyclic loading of 1.2 V with 2 s loading and 2 s unloading.

Movie S2. RBCs respond to static loading of 1.2 V.

Movie S3. Tank-treading motion of an RBC in response to the static loading of 1.2 V.

Movie S4. RBCs respond to an HWR sinusoidal-waveform cyclic loading of 1.2 V with 2 s loading and 2 s unloading.

References

1. Morgan H & Green NG (2003) *AC electrokinetics* (Research Studies Press).
2. Castellarnau M, Errachid A, Madrid C, Juarez A, & Samitier J (2006) Dielectrophoresis as a tool to characterize and differentiate isogenic mutants of Escherichia coli. *Biophysical journal* 91(10):3937-3945.
3. Zheng L, Brody JP, & Burke PJ (2004) Electronic manipulation of DNA, proteins, and nanoparticles for potential circuit assembly. *Biosensors and Bioelectronics* 20(3):606-619.
4. Thom F (2009) Mechanical properties of the human red blood cell membrane at -15 degrees C. *Cryobiology* 59(1):24-27.
5. Gascoyne P*, et al.* (2002) Microsample preparation by dielectrophoresis: isolation of malaria. *Lab on a Chip* 2(2):70-75.
6. Kumar S & Hesketh PJ (2012) Interpretation of ac dielectrophoretic behavior of tin oxide nanobelts using Maxwell stress tensor approach modeling. *Sensors and Actuators B: Chemical* 161(1):1198-1208.
7. Hochmuth RM, Worthy P, & Evans EA (1979) Red cell extensional recovery and the determination of membrane viscosity. *Biophysical journal* 26(1):101-114.
8. Evans EA & Hochmuth RM (1976) A solid-liquid composite model of the red cell membrane. *Journal of Membrane Biology* 30(1):351-362.